Online Resource 1 (ESM_1.pdf)

Supplementary slices, robustness checks, and normalized-stage comparisons for
"Three-Dimensional Flame-Head Bifurcation and Compression–Hydrodynamic Coupling in
LES of Premixed Hydrogen-Air Propagation in a Half-Open Channel".

Flow, Turbulence and Combustion

Youquan Yuan; Jiandong He*

College of Mechanics and Aerospace, Inner Mongolia University of Technology, Hohhot, Inner Mongolia, China

Corresponding author: hjd@imut.edu.cn

This supplementary file contains Fig. S1–S11 and Table S1–S4. The added materials document front-definition robustness, ahead-window sensitivity, wake-window sensitivity, threshold sensitivity, normalized-stage values, and representative-time support data for the $\phi = 0.9$, 1.0, and 1.1 cases.

- Fig. S1–S4: supplementary temperature and velocity slices for $\phi = 0.9$ and $\phi = 1.1$
- Fig. S5–S6: inter-case hydrodynamic and terminal-support comparisons
- Fig. S7–S11: robustness and normalized-stage evidence layer
- Table S1–S4: onset robustness, threshold sensitivity, normalized-stage values, and representative-time support values

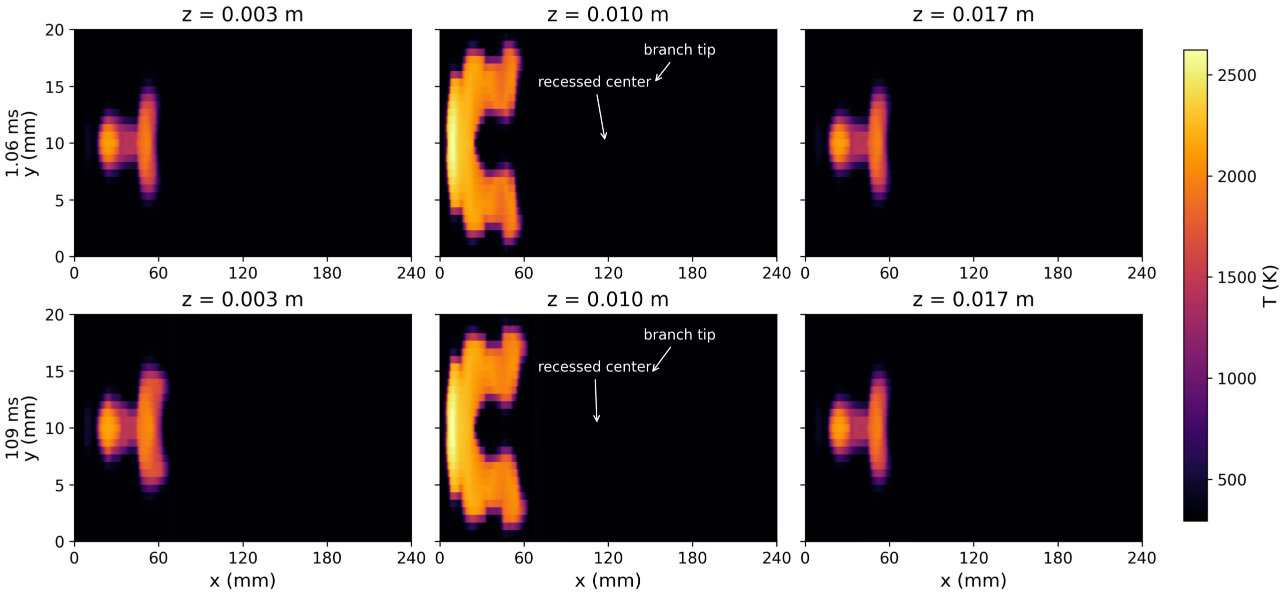

Fig. S1. Temperature slices at three spanwise locations for the lean case with φ = 0.9. The same stratified propagation pattern is observed, but the bifurcation develops later and remains weaker than in the baseline case.

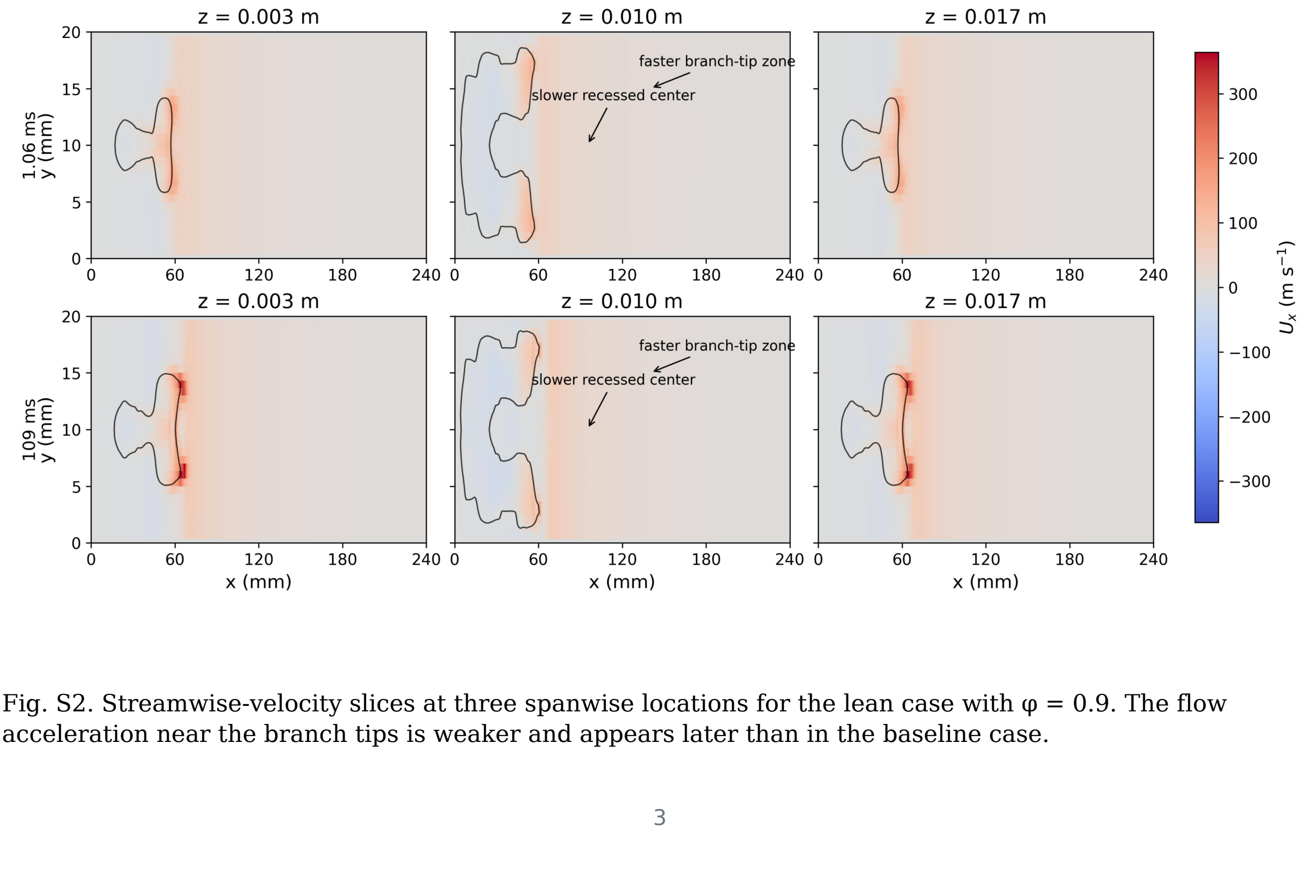

Fig. S2. Streamwise-velocity slices at three spanwise locations for the lean case with φ = 0.9. The flow acceleration near the branch tips is weaker and appears later than in the baseline case.

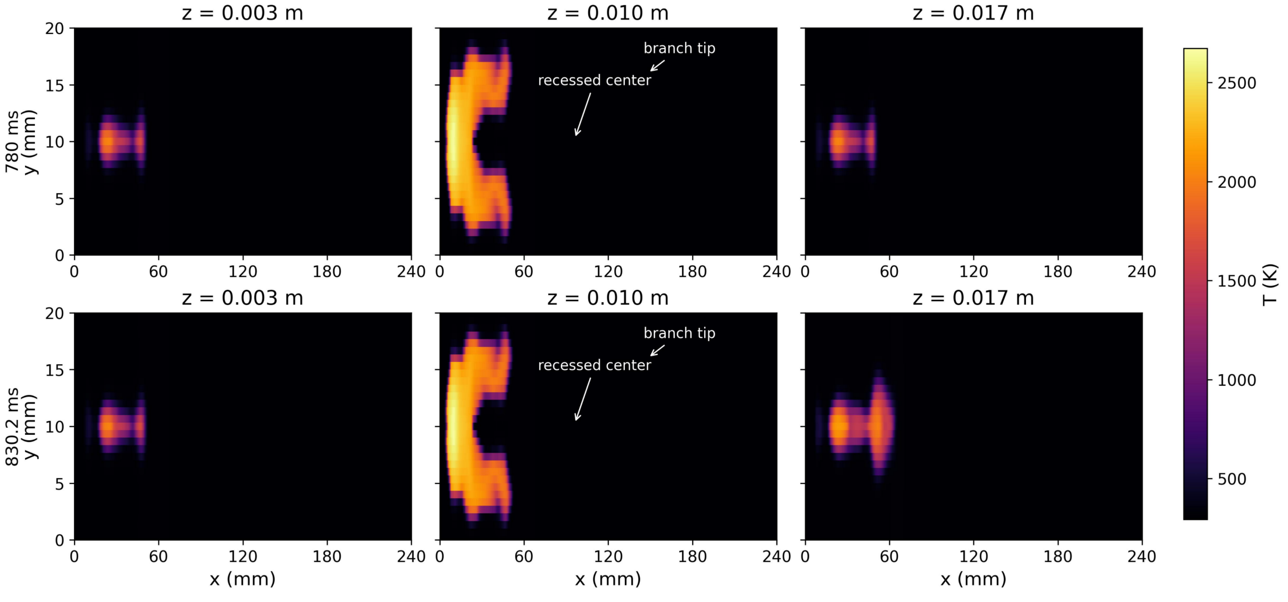

Fig. S3. Temperature slices at three spanwise locations for the richer case with φ = 1.1. The flame-head bifurcation and stratified propagation pattern appear earlier than in the baseline case.

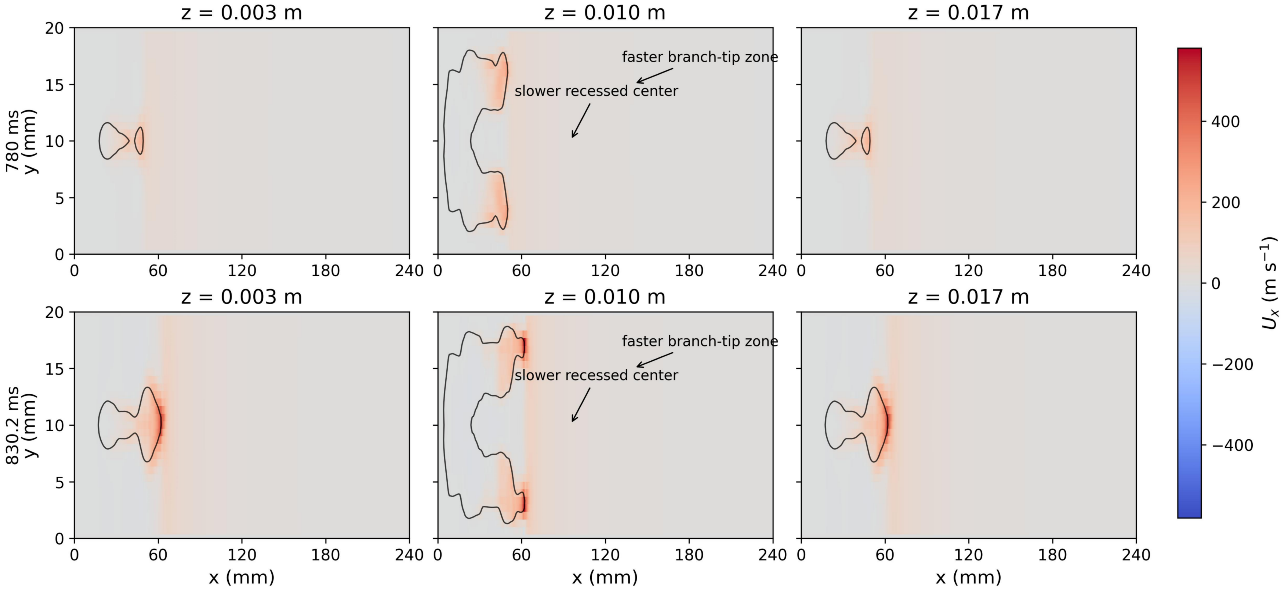

Fig. S4. Streamwise-velocity slices at three spanwise locations for the richer case with φ = 1.1. Strong branch-tip acceleration develops earlier, consistent with the earlier onset of the hydrodynamic precursor regime.

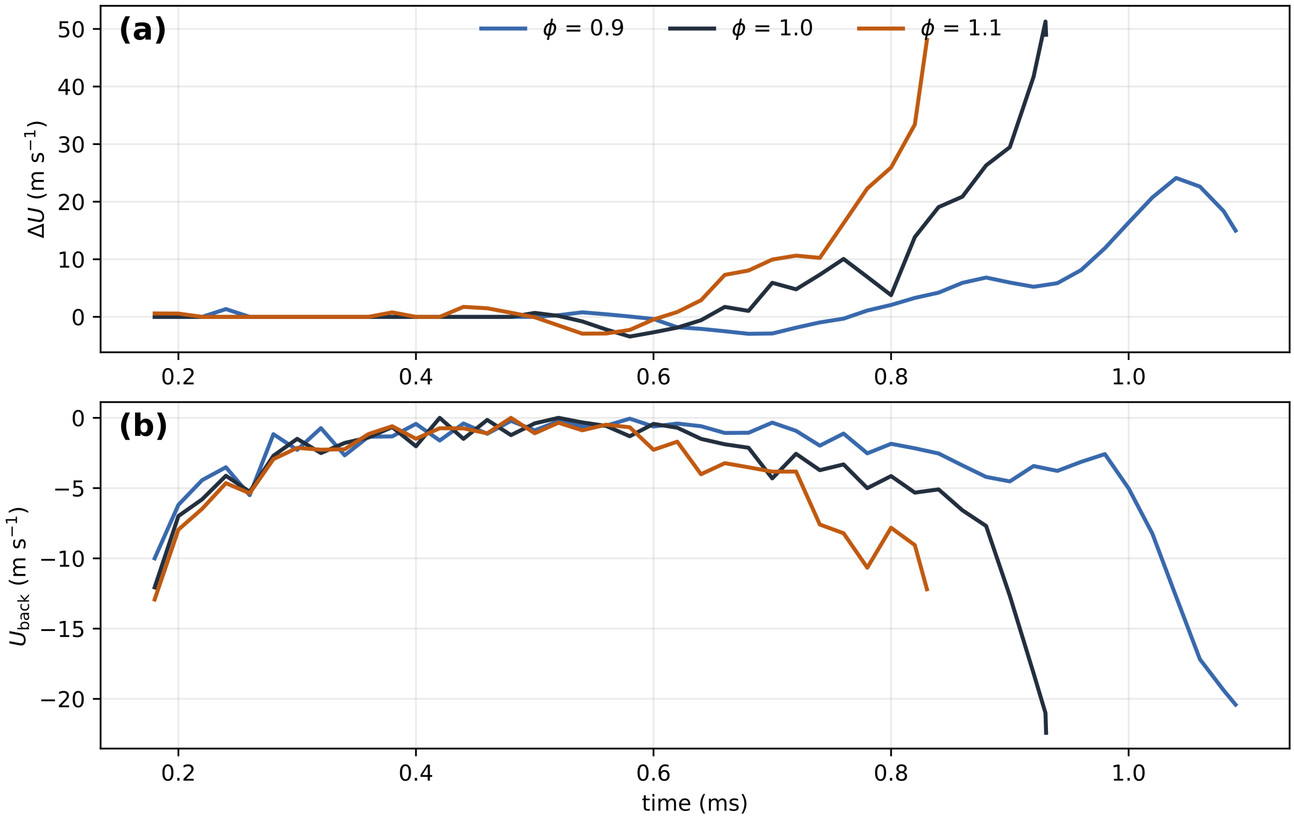

Fig. S5. Supporting comparison of wake-backflow response under different equivalence ratios. The richer and baseline cases develop stronger negative wake velocities earlier than the leaner case, consistent with the earlier transition into the coupled precursor regime.

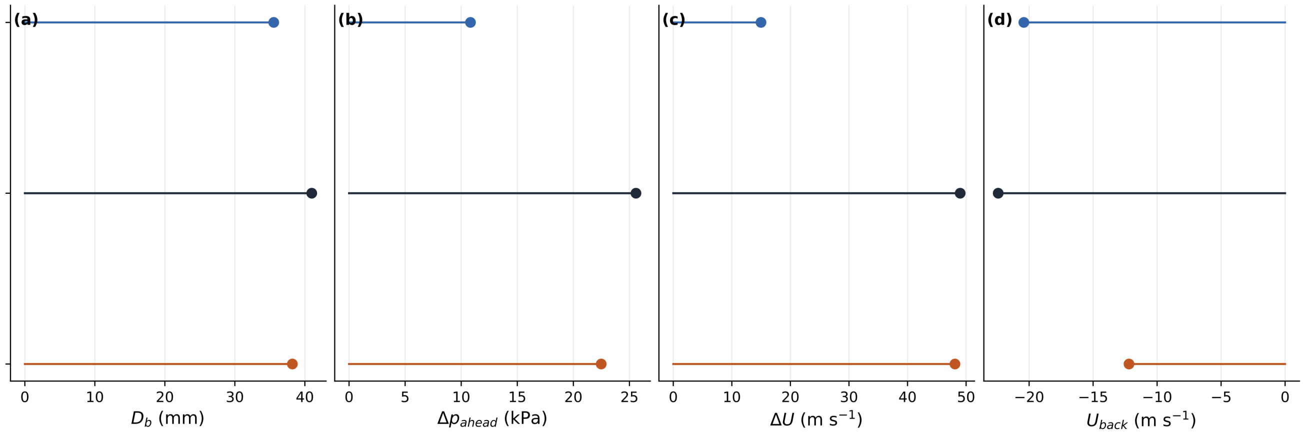

Fig. S6. Terminal comparison of the principal precursor quantities under different equivalence ratios, including D_b, Δp_{ahead}, ΔU, and U_{back}.

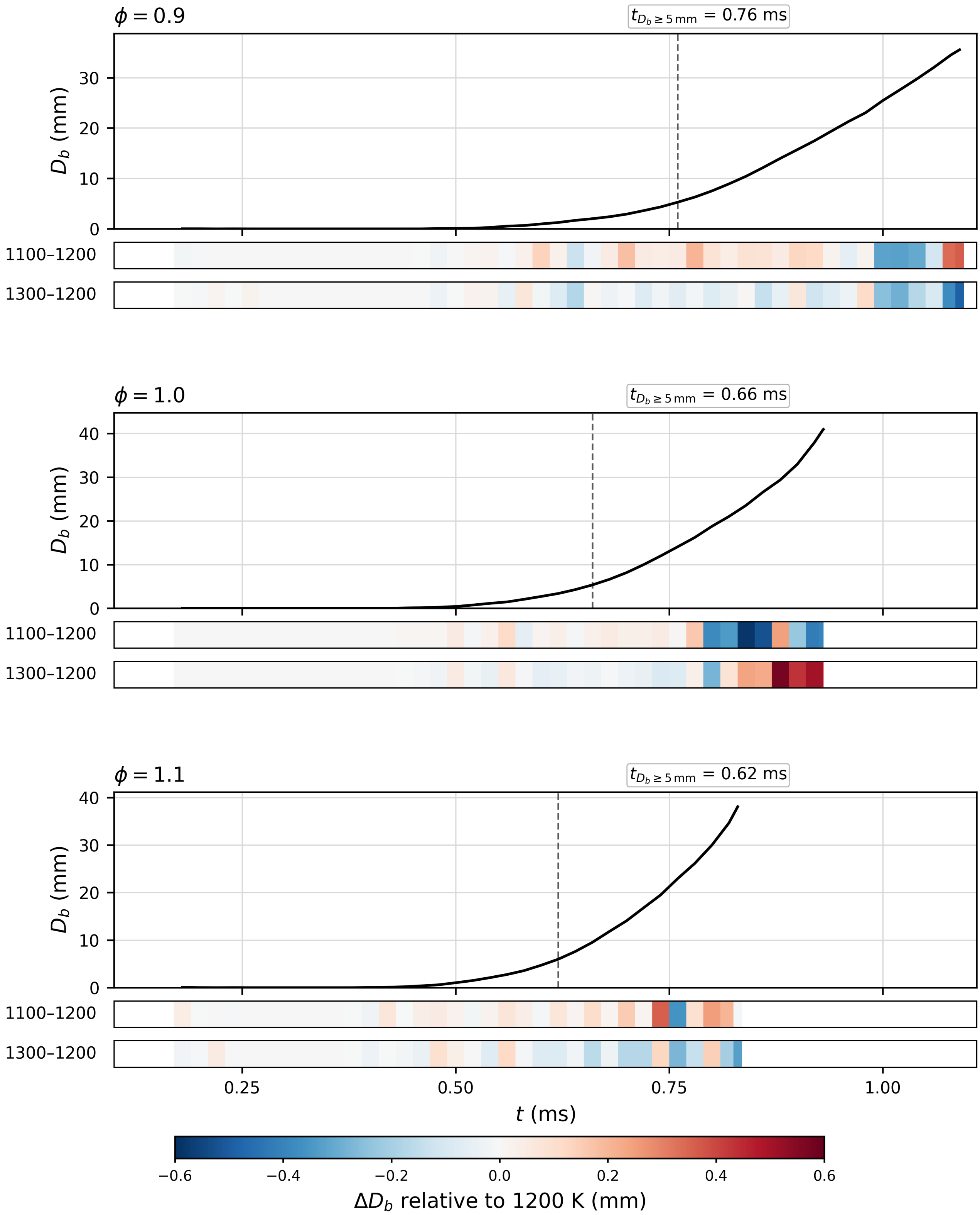

Fig. S7. Sensitivity of D_b to the front definition. For each case, the formal bifurcation depth was recalculated from center-plane contours defined by T = 1100, 1200, and 1300 K. Neighboring front definitions produce only limited changes in magnitude, while the inter-case ordering and onset timing remain unchanged.

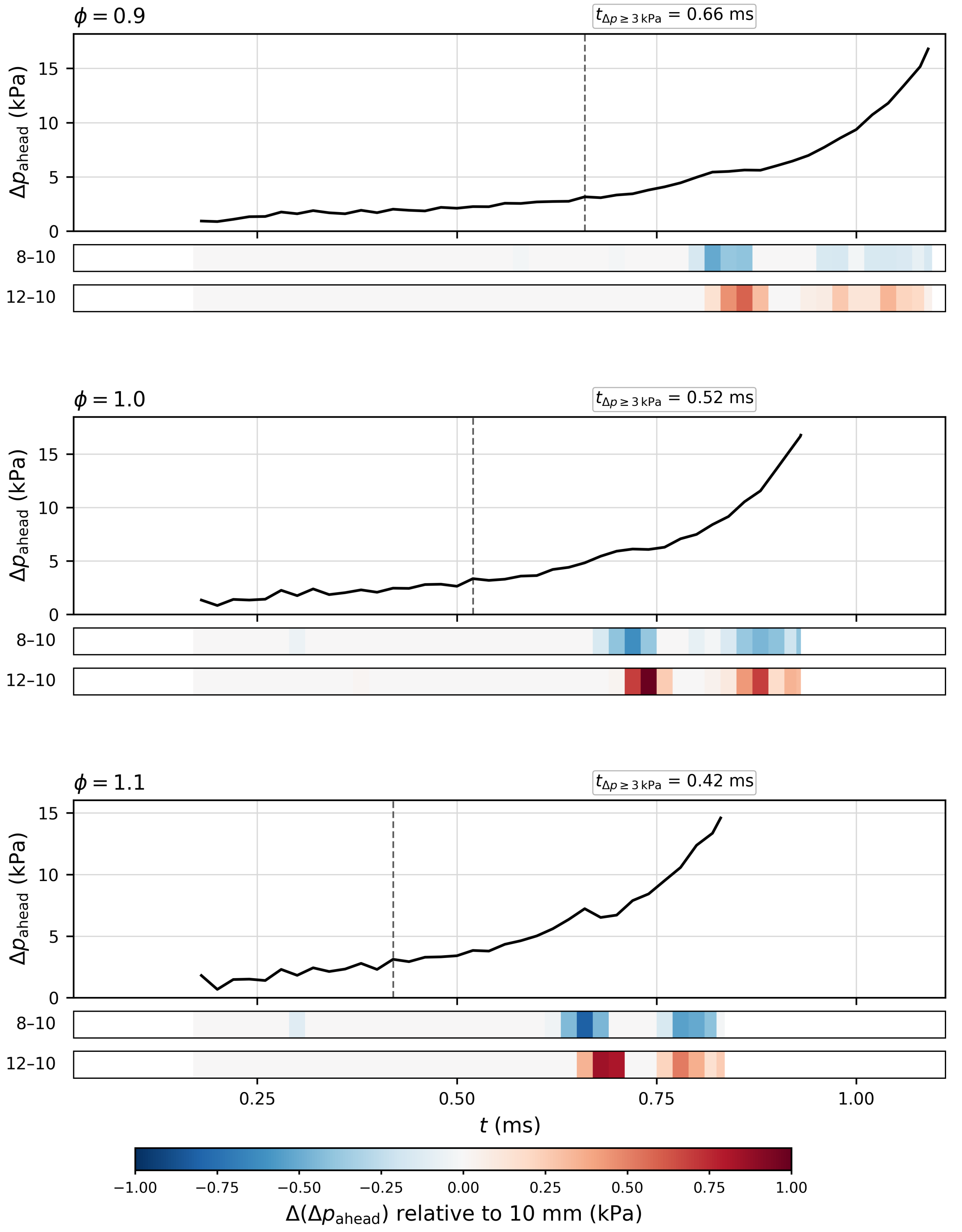

Fig. S8. Sensitivity of $\Delta p_{\mathrm{ahead}}$ to the ahead-window length. The pressure metric was recomputed over $[x_{\mathrm{center}}, x_{\mathrm{center}} + 8\ \mathrm{mm}]$, $[x_{\mathrm{center}}, x_{\mathrm{center}} + 10\ \mathrm{mm}]$, and $[x_{\mathrm{center}}, x_{\mathrm{center}} + 12\ \mathrm{mm}]$ with $p_0 = 101325$ Pa. The absolute values vary modestly, but the onset ordering remains unchanged.

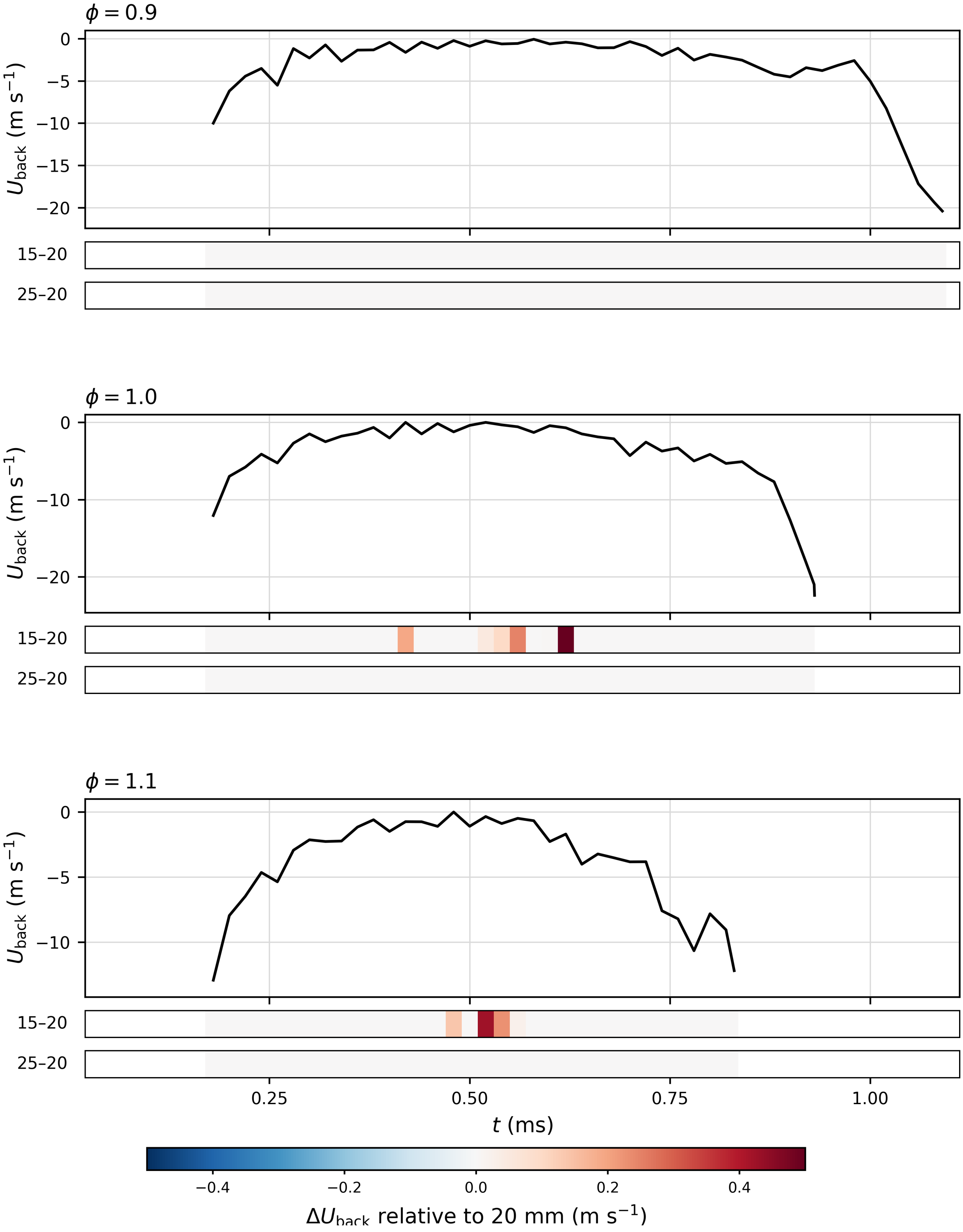

Fig. S9. Sensitivity of U_{back} to the wake-window length. The wake-backflow metric was recomputed over $[\max(0, x_{center} - 15\text{ mm}), x_{center}]$, $[\max(0, x_{center} - 20\text{ mm}), x_{center}]$, and $[\max(0, x_{center} - 25\text{ mm}), x_{center}]$. The magnitude changes with window length, but the qualitative evolution is preserved.

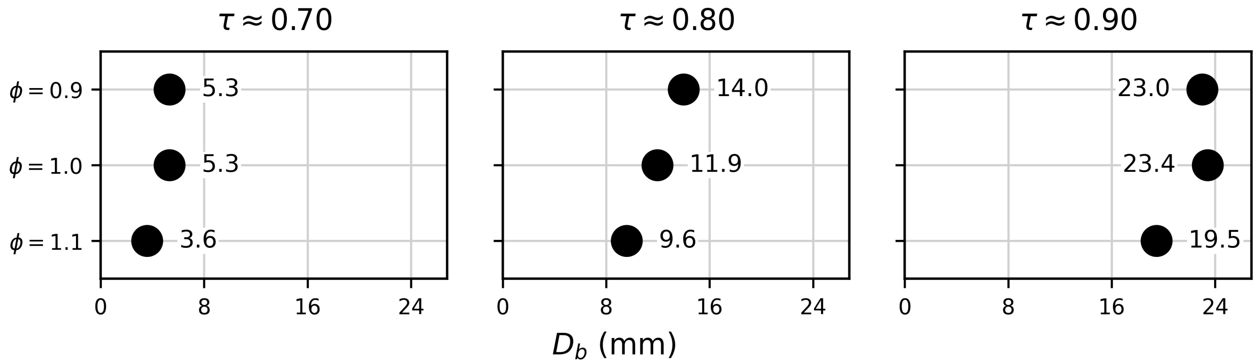

Fig. S10. Normalized-stage comparison of D_b at matched $\tau \approx 0.70$, 0.80, and 0.90. The three cases remain separated after normalization, and the stoichiometric case retains the strongest late-stage structural amplification.

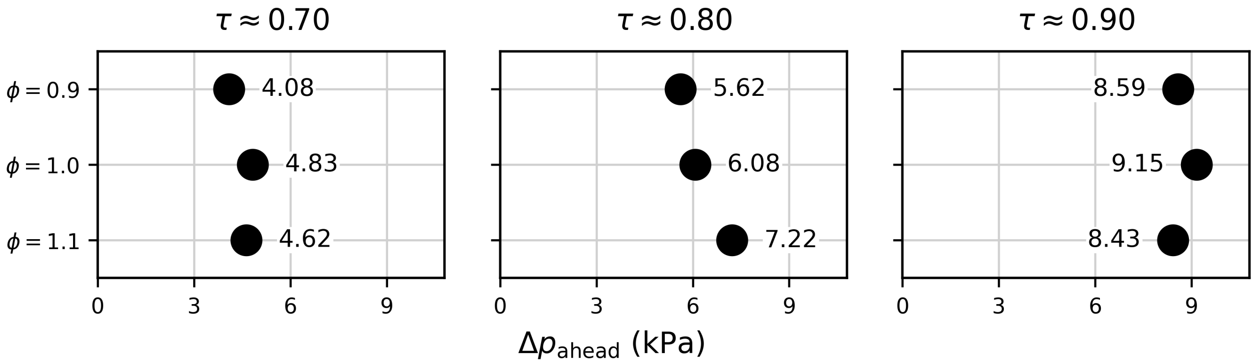

Fig. S11. Normalized-stage comparison of Δp_{ahead} at matched $\tau \approx 0.70$, 0.80, and 0.90. The cases remain distinguishable after normalization, showing that equivalence ratio affects not only the total stable duration but also the internal distribution of the compression response.

Table S1. Event/onset robustness across neighboring front definitions and window choices.

For each case, the baseline definition is compared against alternative front levels and modest ahead/wake window variations. The inter-case ordering is unchanged in all listed scenarios.

case	φ	scenario	front level (K)	ahead (mm)	wake (mm)	t(D_b≥5) (ms)	t(Δp≥3) (ms)	t_last (ms)
phi0p9	0.9	baseline	1200	10	20	0.76	0.66	1.09
phi0p9	0.9	front 1100 K	1100	10	20	0.76	0.66	1.09
phi0p9	0.9	front 1300 K	1300	10	20	0.76	0.66	1.09
phi0p9	0.9	ahead 8 mm	1200	8	20	0.76	0.66	1.09
phi0p9	0.9	ahead 12 mm	1200	12	20	0.76	0.66	1.09
phi0p9	0.9	wake 15 mm	1200	10	15	0.76	0.66	1.09
phi0p9	0.9	wake 25 mm	1200	10	25	0.76	0.66	1.09
phi1p0	1	baseline	1200	10	20	0.66	0.52	0.931
phi1p0	1	front 1100 K	1100	10	20	0.66	0.52	0.931
phi1p0	1	front 1300 K	1300	10	20	0.66	0.52	0.931
phi1p0	1	ahead 8 mm	1200	8	20	0.66	0.52	0.931
phi1p0	1	ahead 12 mm	1200	12	20	0.66	0.52	0.931
phi1p0	1	wake 15 mm	1200	10	15	0.66	0.52	0.931
phi1p0	1	wake 25 mm	1200	10	25	0.66	0.52	0.931
phi1p1	1.1	baseline	1200	10	20	0.62	0.42	0.83
phi1p1	1.1	front 1100 K	1100	10	20	0.62	0.42	0.83
phi1p1	1.1	front 1300 K	1300	10	20	0.62	0.42	0.83
phi1p1	1.1	ahead 8 mm	1200	8	20	0.62	0.42	0.83
phi1p1	1.1	ahead 12 mm	1200	12	20	0.62	0.42	0.83
phi1p1	1.1	wake 15 mm	1200	10	15	0.62	0.42	0.83
phi1p1	1.1	wake 25 mm	1200	10	25	0.62	0.42	0.83

Table S2. Threshold sensitivity for the operational onset markers.

Event times remain ordered as φ = 1.1 earliest, φ = 1.0 intermediate, and φ = 0.9 latest across the threshold variations listed here.

case	φ	t(D_b≥4) (ms)	t(D_b≥5) (ms)	t(D_b≥6) (ms)	t(Δp≥2.5) (ms)	t(Δp≥3.0) (ms)	t(Δp≥3.5) (ms)
phi0p9	0.9	0.74	0.76	0.78	0.56	0.66	0.74
phi1p0	1	0.64	0.66	0.68	0.46	0.52	0.58
phi1p1	1.1	0.6	0.62	0.62	0.38	0.42	0.52

Table S3. Normalized-stage values at τ ≈ 0.70, 0.80, and 0.90.

The tabulated values support the normalized-stage dot plots in Fig. S10 and Fig. S11 and show that the three cases do not collapse to a single scaled evolution.

case	φ	τ target	τ nearest	time (ms)	D_b (mm)	Δp_ahead (kPa)	ΔU (m/s)	U_back (m/s)
phi0p9	0.9	0.7	0.697	0.76	5.322	4.085	-0.309	-1.121
phi0p9	0.9	0.8	0.807	0.88	13.99	5.615	6.826	-4.204
phi0p9	0.9	0.9	0.899	0.98	23	8.585	11.92	-2.582
phi1p0	1	0.7	0.709	0.66	5.316	4.825	1.727	-1.882
phi1p0	1	0.8	0.795	0.74	11.95	6.075	7.32	-3.723
phi1p0	1	0.9	0.903	0.84	23.43	9.155	19.06	-5.091
phi1p1	1.1	0.7	0.699	0.58	3.583	4.625	-2.267	-0.67
phi1p1	1.1	0.8	0.795	0.66	9.578	7.225	7.292	-3.225
phi1p1	1.1	0.9	0.891	0.74	19.47	8.425	10.25	-7.592

Table S4. Representative-time robustness / support table at matched normalized stages.

Values are reported for the matched τ stages used in the normalized comparison. D_b columns are in mm, Δp columns are in kPa, and U_back columns are in m/s.

case	φ	τ target	τ nearest	time (ms)	D_b 1100	D_b 1200	D_b 1300	ΔD_b 1100−1200	ΔD_b 1300−1200	Δp 8	Δp 10	Δp 12	U_back 15	U_back 20	U_back 25
phi0p9	0.9	0.7	0.697	0.76	5.342	5.291	5.221	0.051	-0.07	4.085	4.085	4.085	-1.121	-1.121	-1.121
phi0p9	0.9	0.8	0.807	0.88	14.03	13.98	13.93	0.051	-0.051	5.615	5.615	5.925	-4.204	-4.204	-4.204
phi0p9	0.9	0.9	0.899	0.98	23.07	23.05	23.16	0.023	0.114	8.415	8.585	8.855	-2.582	-2.582	-2.582
phi1p0	1	0.7	0.709	0.66	5.374	5.344	5.315	0.029	-0.029	4.825	4.825	4.825	-1.882	-1.882	-1.882
phi1p0	1	0.8	0.795	0.74	12.04	11.98	11.9	0.049	-0.085	5.685	6.075	7.065	-3.723	-3.723	-3.723
phi1p0	1	0.9	0.903	0.84	22.99	23.57	23.81	-0.584	0.24	9.005	9.155	9.255	-5.091	-5.091	-5.091
phi1p1	1.1	0.7	0.699	0.58	3.621	3.581	3.57	0.04	-0.011	4.625	4.625	4.625	-0.67	-0.67	-0.67
phi1p1	1.1	0.8	0.795	0.66	9.636	9.533	9.373	0.103	-0.16	6.405	7.225	7.575	-3.225	-3.225	-3.225
phi1p1	1.1	0.9	0.891	0.74	19.87	19.51	19.64	0.36	0.131	8.425	8.425	8.425	-7.592	-7.592	-7.592